35th Annual International Conference of the IEEE EMBS
Osaka, Japan, 3 - 7 July, 2013

Cellular Automaton Model for Simulating Tissue-Specific Intestinal Electrophysiological Activity

Jerry Gao, Peng Du, Greg O'Grady, Rosalind Archer, Simon J. Gibbons, Gianrico Farrugia, and Leo K. Cheng

Abstract— **Depletion of interstitial cell of Cajal (ICC) networks is known to occur in various gastrointestinal (GI) motility disorders. Although techniques for quantifying the structure of ICC networks are available, the ICC network structure-function relationships are yet to be well elucidated. Existing methods of relating ICC structure to function are computationally expensive, and it is difficult to up-scale them to larger multiscale simulations. A new cellular automaton model for simulating tissue-specific slow wave propagation was developed, and in preliminary studies the automaton model was applied on jejunal ICC network structures from wild-type and 5-HT_{2B} receptor knockout (ICC depleted) mice. Two metrics were also developed to quantify the simulated propagation patterns: 1) ICC and 2) non-ICC activation lag metrics. These metrics measured the average delay in time taken for the slow wave to propagate across the ICC and non-ICC domain throughout the entire network compared to the theoretical fastest propagation, respectively. Slow wave propagation was successfully simulated across the ICC networks with greatly reduced computational time compared to previous methods, and the propagation pattern metrics quantitatively revealed an impaired propagation during ICC depletion. In conclusion, the developed slow wave propagation model and propagation pattern metrics offer a computationally efficient framework for relating ICC structure to function. These tools can now be further applied to define ICC structure-function relationships across various spatial and temporal scales.**

I. Introduction

Gastrointestinal (GI) motility is facilitated by specialized cells called interstitial cells of Cajal (ICC) [1, 2]. Various populations of ICC exist throughout the GI tract [3], and these different populations also play different functional roles [4]. In particular, in the upper gut, ICC from the myenteric plexus (ICC-MP) between the longitudinal and circular smooth muscle layers act as the primary pacemaker cells responsible for initiating and propagating an underlying omnipresent electrophysiological activity, termed 'slow waves', for coordinating motility in the intestine [5, 6]. This activity is similar to that generated by cardiac pacemaker cells [7].

ICC loss and injury is now recognized as a major contributor to several GI motility disorders, including gastroparesis [8], slow transit constipation [9], and intestinal pseudo-obstruction [10]. However, the functional significance of ICC depletion remains speculative, partly due to the lack of methods for quantitatively analyzing ICC structure-function relationships. To address this issue, we previously developed numerical metrics to quantify structural properties of ICC networks [11], and now further techniques for relating the quantified structure to function is required.

Previous studies have simulated tissue-specific slow wave propagation over ICC networks by coupling imaging data with a modified biophysically-based Corrias and Buist cell model [12] embedded within a continuum modeling framework [11, 13]. However, this methodology is computationally expensive [13], mainly due to the large number of equations and parameters present in the cell model, and hence difficulties exist in up-scaling these simulations to larger multiscale simulation studies. An alternative strategy of implementing cellular automaton models to simulate slow wave propagation has also been previously conducted [14, 15], but these previous studies focused on a larger spatial scale and did not incorporate structural detail from real ICC networks.

In this study, we present a new cellular automaton model for simulating the activation phase of slow wave propagation over tissue-specific ICC networks, as well as numerical metrics for quantitatively measuring the observed propagation patterns. To demonstrate proof-of-concept, these tools were then applied to assess the differences in function between normal and depleted ICC networks from the jejunum of a mouse model of intestinal ICC depletion.

II. Methods

A. Cellular Automaton Model

The cellular automaton model simulated the activation phase of slow wave propagation over a 2D grid-structure domain by taking discrete time-steps. The individual grid nodes were separated into ICC and non-ICC types, and the simulated slow wave propagation was defined by activation values a between 0 and 1 at the node positions. The activation value is representative of the membrane potential, with 0 representing the resting membrane potential ('off'), and 1 representing the peak membrane potential ('on'). As the model focused on the activation phase only, no further activity occurred for a node

Manuscript received 18 January, 2013. J. Gao is supported by a University of Auckland Heath Research Doctoral Scholarship, a Freemasons Postgraduate Scholarship, and a R. H. T. Bates Postgraduate Scholarship. P. Du is supported by a Rutherford Foundation New Zealand Postdoctoral Fellowship and a Marsden Fast-Start Grant. This work is funded in part by grants from the New Zealand Health Research Council, and National Institutes of Health grants (DK57061, DK68055, and DK64775).

J. Gao, P. Du, and L. K. Cheng are with the Auckland Bioengineering Institute, The University of Auckland, Auckland, New Zealand (phone: 649-373-7599; fax: 649-367-7157; e-mail: l.cheng@auckland.ac.nz).

G. O'Grady is with the Auckland Bioengineering Institute and the Department of Surgery, The University of Auckland, Auckland, New Zealand.

R. Archer is with the Department of Engineering Science, The University of Auckland, Auckland, New Zealand.

S. Gibbons and G. Farrugia are with the Enteric Neuroscience Program, Division of Gastroenterology and Hepatology, Mayo Clinic College of Medicine, Rochester, MN, USA.

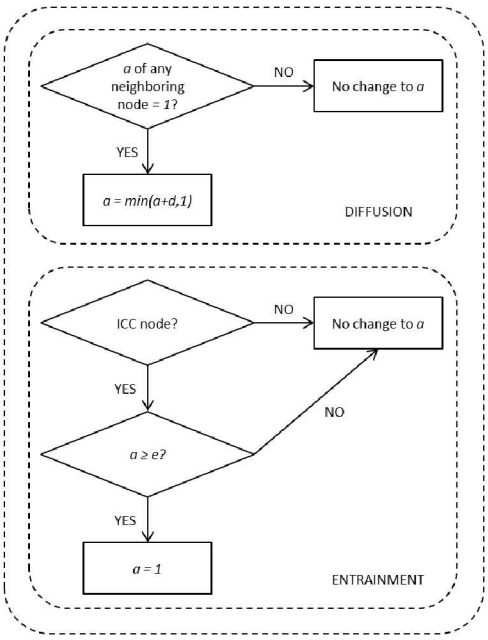

Figure 1. Schematic diagram of the cellular automaton model, showing the decision processes of the two model components performed every time-step to update individual nodal activation values. a is the activation value of the node currently being considered unless otherwise specified, and d and e are the diffusion and entrainment parameters described further in the text.

once it switched to the 'on' state. The model contained the following two components (Fig. 1):

1) Diffusion: This component modeled the passive diffusion effect of membrane potential. Regardless of node type (ICC or non-ICC), all 'on' nodes increased the activation values of immediate neighboring nodes by the diffusion rate parameter d per time-step until these neighboring nodes were also switched to the 'on' state (i.e., the activation value reached the maximum of 1).

2) Entrainment: Isolated ICC spontaneously generate slow waves at their own intrinsic frequencies [16], but in intact tissue ICC are organized in an electrical syncytium, and the cells become 'entrained' to generate activity matching the highest frequency present in the syncytium [17]. This component modeled this ICC characteristic. If at any time-step an ICC node possessed an activation value above the entrainment threshold parameter e, the node was immediately switched to the 'on' state.

B. Simulation Setup

Slow wave propagation was simulated over six ICC-MP networks from the jejunum of 4-week-old wild-type (WT) and 5-HT_{2B} receptor knockout (KO) mice respectively. Normally, serotonin acts on the 5-HT_{2B} receptors to increase ICC proliferation, and a lack of these receptors results in ICC depletion [18]. Two dimensional bitmaps of the network structures were obtained from confocal imaging data as previously described [13, 18], and were then oriented such that the longitudinal axis of the intestine was vertical (Fig. 2). These structures represented physical dimensions of 225×225 μm with 362×362 pixels, and each pixel was mapped to a node in the cellular automaton model to determine the node type (ICC or non-ICC). Therefore, note that numerous ICC nodes would be used to represent a single physical cell.

As an initial stimulus to the simulations, all ICC nodes in the top row of the grid-structure were prescribed to the 'on' state at time t = 0 ms. This imitated a planar slow wave wavefront traveling along the length of the intestine. Slow wave propagation was simulated with a time-step of 0.1 ms until all nodes were switched 'on'. Simulation parameters d and e were both arbitrarily selected to be 0.1, and hence given an 'on' neighboring node, $switch_{NICC}$ and $switch_{ICC}$, the times required to switch non-ICC and ICC nodes from the 'off' to 'on' state were 1 ms and 0.1 ms respectively.

C. Propagation Pattern Metrics

In order to quantitatively compare the resulting slow wave propagation patterns simulated over different network structures, two numerical metrics were developed: the ICC and non-ICC activation lag metrics. These metrics measured, in ms, the average time delay in simulated activation times (AT, i.e., the times at which a node switched to the 'on' state) from the theoretical minimum AT of the ICC and non-ICC nodes across the entire network, respectively. That is, the differences between simulated and theoretical minimum AT were calculated for each node, and an average value for each of the node types was computed. The theoretical minimum AT for the ICC and non-ICC nodes were defined as follows for the simulation setup of this study:

1) Minimum ICC AT ($minAT_{ICC}$): ICC nodes in the top row were prescribed to 'on' as an initial stimulus, and hence these nodes had a theoretical minimum AT of 0 ms. As the diffusion component of the model responsible for the spread of propagation only considered immediate neighboring nodes, it is only possible to switch 'on' a further row of ICC nodes every 0.1 ms ($switch_{ICC}$). Therefore, the theoretical minimum AT of ICC nodes can be computed as

$$minAT_{ICC} = 0.1 \times (n_{row}-1), \quad (1)$$

where n_{row} is the row number starting with 1 at the top row.

2) Minimum non-ICC AT ($minAT_{NICC}$): Both the top and second-to-top rows were immediate neighboring nodes to the initial ICC node stimulus, and hence the theoretical minimum AT for non-ICC nodes in these rows were 1 ms ($switch_{NICC}$). As the slow wave propagated faster through ICC, assuming a pathway of ICC nodes was available to activate the non-ICC nodes in the subsequent rows below, each additional row delayed the theoretical minimum AT by 0.1 ms ($switch_{ICC}$). Therefore, the theoretical minimum AT of non-ICC nodes can be computed as

$$minAT_{NICC} = 0.1 \times max(n_{row}-2,0)+1. \quad (2)$$

III. Results

A. Slow Wave Propagation Simulation

The activation phase of slow wave propagation was successfully simulated over tissue-specific ICC network structures using the developed cellular automaton model (Fig. 3). It took on average 49.6±1.5 ms and 60.0±4.1 ms (±1 standard error) for the slow wave to propagate across the entire WT and KO networks (i.e., for all nodes to switch to the 'on' state) respectively. The computational time required to

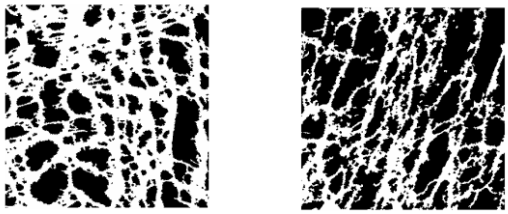

Figure 2. Example WT (left) and KO (right) ICC networks with the longitudinal axis of the intestine aligned vertically. These networks represented physical dimensions of 225×225 µm with 362×362 pixels. White represents ICC, whereas black represents non-ICC.

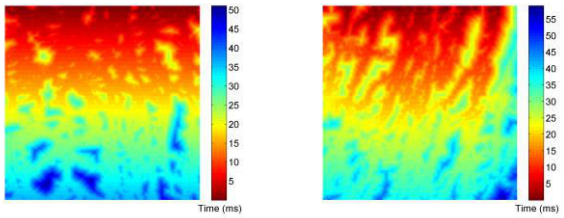

Figure 3. AT maps of simulated slow wave propagation over WT (left) and KO (right) ICC networks as shown in Fig. 2. The gradient of colors show the AT throughout the network, with red and blue indicating early and late activations respectively.

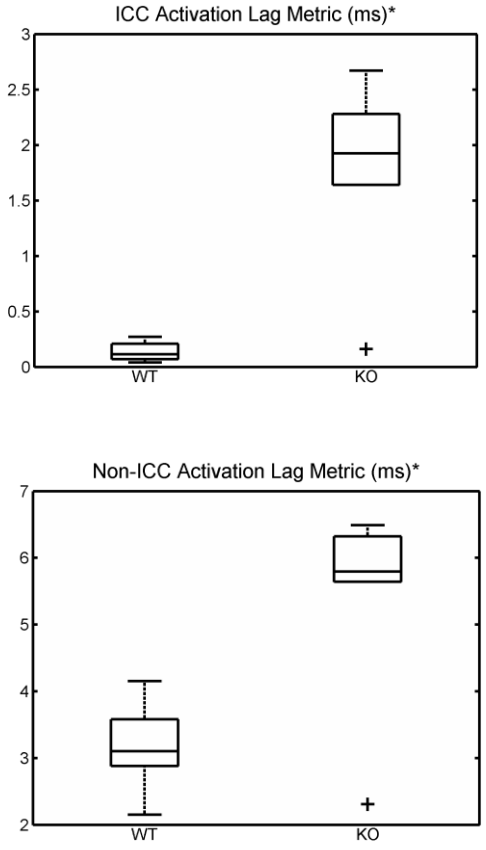

Figure 4. Propagation pattern metric values of simulated slow wave propagation over WT and KO ICC networks. A * in the title indicates a statistically significant difference ($p<0.01$). A + in the boxplot indicates an outlier.

simulate slow wave propagation over a single network was approximately 3.5 s on a quad-core Intel® Xeon® W3530 CPU.

B. *Propagation Pattern Metrics*

The propagation pattern metric values of simulated slow wave propagation over the WT and KO networks are plotted in Fig. 4. These data showed that slow wave propagation over KO networks had on average a 14 times higher ICC activation lag metric value ($p<0.01$) and a 90% higher non-ICC activation lag metric value ($p<0.01$) compared to that over WT networks.

IV. Discussion

A cellular automaton model for simulating the activation phase of slow wave propagation over tissue-specific ICC networks was developed, and as proof-of-concept this model was used to simulate slow wave propagation over normal and depleted murine jejunal ICC networks. Two numerical metrics for quantifying propagation patterns were also developed and used to contrast the simulated propagation patterns over the WT and KO networks. These simulations and metrics showed with quantitative evidence that ICC depletion impaired propagation of slow waves across the network structure. These preliminary results are consistent with, and may help to explain, recent data on slow wave propagation from patients with gastroparesis, a disorder in which the stomach fails to empty normally. ICC depletion in these patients has been found to be associated with reduced slow wave propagation velocities down the stomach [8]. Note that the formulations of the propagation pattern metrics were not biased by the ratio of ICC to non-ICC nodes. There is no direct relationship between the propagation pattern metrics and the ICC to non-ICC node ratio, so networks of different node ratios can still have the same metric values. Therefore, in the simulation, the quantified impairment in propagation over the KO networks was not purely a side-effect of less ICC nodes, but rather a feature of degradation of the network structure.

The cellular automaton model developed here provides a computationally efficient tool for modeling tissue-specific slow wave propagation in multiscale simulations. This model differs from previous slow wave propagation cellular automaton models [14, 15] in that both ICC and non-ICC node types were explicitly represented, and appropriate cellular automaton rules were applied accordingly. This facilitates investigations of structure on function at much higher spatial resolutions, which is necessary to capture the ICC network structure. The model also produced streamlined results with the previous method of embedding biophysically-based cell models within a continuum modeling framework [13], but with greatly reduced computational expenses. Although not directly comparable, the previous method took 2 h to simulate 400 ms of slow wave propagation over network structures defined by 262,144 nodes [13], whereas the simulations here only took 3.5 s to simulate approximately 60 ms of slow wave propagation over network structures defined by 131,044 nodes. Assuming simulation length and number of nodes is linearly proportional to computational time, this corresponds to a speed-up of over 150 times. Further studies with a standardized modeling setup will be required to formally discern the similarity and differences between the different modeling strategies.

The developed cellular automaton model worked in time-steps, and the time-step value was essentially a scaling factor to the simulation output. However, for the simulated propagation to be physiologically realistic temporally, the selection of the time-step value was critical. In the current simulation setup, it took a minimum of 361 time-steps to simulate propagation through a distance of 225 µm (the longitudinal dimension of the networks). The time-step value of 0.1 ms was selected such that the maximum propagation speed across the networks was 6 mms^{-1}, similar to that experimentally recorded in the rat jejunum [14].

The slow wave propagation simulations in this study are still relatively simplistic in comparison to the real physiological activity. Basic cellular automaton rules were implemented in the slow wave propagation model to exhibit the general behavior of only the diffusion and entrainment mechanisms; the model parameters (*d* and *e*) were arbitrarily chosen; and the horizontally uniform initial stimulus to the simulations did not account for potential upstream effects (i.e., influence of network structures above the current field of view). However, as the simulations were all performed under a consistent setup, we believe the quantified differences in slow wave propagation over the normal and depleted ICC networks remain valid. Following the calibration of the model and simulation setup using results obtained from previous modeling strategies and experimental tissue-specific electrophysiological data, this proposed modeling framework may transform into a powerful predictive tool.

V. Conclusion

This study presented a new tissue-specific slow wave propagation model and numerical metrics for quantifying slow wave propagation patterns. Together, these tools in conjunction provide a computationally efficient framework for relating ICC structure to function, and initial findings have quantified the degree of propagation impairment occurring in ICC depletion. This methodology can now be further applied to define structure-function relationships in ICC networks across various spatial and temporal scales.

As shown experimentally, segmentation of the ICC networks in-vivo enables the intrinsic frequency of activity in distal parts of the network to be expressed [16]. In the future, an intrinsic component could be included in the model to examine the complex interactions between these different propagation mechanisms. The model and simulation setup can also be calibrated against previous modeling strategies and experimental data to improve the validity of the simulations.

Acknowledgment

The authors would like to thank Dr. Vivek Tharayil for his assistance with the immunohistochemistry for detecting ICC.

References

[1] G. Farrugia, "Interstitial cells of Cajal in health and disease," *Neurogastroenterol Motil,* vol. 20, pp. 54-63, 2008.

[2] C. J. Streutker, J. D. Huizinga, D. K. Driman, and R. H. Riddell, "Interstitial cells of Cajal in health and disease. Part I: normal ICC structure and function with associated motility disorders," *Histopathology,* vol. 50, pp. 176-189, 2007.

[3] M. Hanani, G. Farrugia, and T. Komuro, "Intercellular coupling of interstitial cells of Cajal in the digestive tract," *Int Rev Cytol,* vol. 242, pp. 249-282, 2005.

[4] R. Lees-Green, P. Du, G. O'Grady, A. Beyder, G. Farrugia, and A. J. Pullan, "Biophysically based modeling of the interstitial cells of Cajal: current status and future perspectives," *Front Physiol,* vol. 2, 2011.

[5] J. D. Huizinga, L. Thuneberg, M. Klüppel, J. Malysz, H. B. Mikkelsen, and A. Bernstein, "W/kit gene required for interstitial cells of Cajal and for intestinal pacemaker activity," *Nature,* vol. 373, pp. 347-349, 1995.

[6] T. Seerden, W. Lammers, B. De Winter, J. De Man, and P. Pelckmans, "Spatiotemporal electrical and motility mapping of distension-induced propagating oscillations in the murine small intestine," *Am J Physiol Gastrointest Liver Physiol,* vol. 289, pp. G1043-G1051, 2005.

[7] A. Katz, *Physiology of the Heart*, 5th ed. Philadelphia, USA: Lippincott Williams & Wilkins, 2011.

[8] G. O'Grady, T. R. Angeli, P. Du, C. Lahr, W. J. E. P. Lammers, J. A. Windsor, T. L. Abell, G. Farrugia, A. J. Pullan, and L. K. Cheng, "Abnormal initiation and conduction of slow-wave activity in gastroparesis, defined by high-resolution electrical mapping," *Gastroenterology,* vol. 143, pp. 589-598, 2012.

[9] T. Wedel, J. Spiegler, S. Soellner, U. J. Roblick, T. H. Schiedeck, H. P. Bruch, and H. J. Krammer, "Enteric nerves and interstitial cells of Cajal are altered in patients with slow-transit constipation and megacolon," *Gastroenterology,* vol. 123, pp. 1459-1467, 2002.

[10] A. E. Feldstein, S. M. Miller, M. El-Youssef, D. Rodeberg, N. M. Lindor, L. J. Burgart, J. H. Szurszewski, and G. Farrugia, "Chronic intestinal pseudoobstruction associated with altered interstitial cells of Cajal networks," *J Pediatr Gastroenterol Nutr,* vol. 36, pp. 492-497, 2003.

[11] J. Gao, P. Du, R. Archer, G. O'Grady, S. J. Gibbons, G. Farrugia, L. K. Cheng, and A. J. Pullan, "A stochastic multi-scale model of electrical function in normal and depleted ICC networks," *IEEE Trans Biomed Eng,* vol. 58, pp. 3451-3455, 2011.

[12] A. Corrias and M. L. Buist, "Quantitative cellular description of gastric slow wave activity," *Am J Physiol Gastrointest Liver Physiol,* vol. 294, pp. G989-G995, 2008.

[13] P. Du, G. O'Grady, S. J. Gibbons, R. Yassi, R. Lees-Green, G. Farrugia, L. K. Cheng, and A. J. Pullan, "Tissue-specific mathematical models of slow wave entrainment in wild-type and 5-HT(2B) knockout mice with altered interstitial cells of Cajal networks," *Biophys J,* vol. 98, pp. 1772-1781, 2010.

[14] W. J. E. P. Lammers, H. M. Al-Bloushi, S. A. Al-Eisaei, F. A. Al-Dhaheri, B. Stephen, R. John, S. Dhanasekaran, and S. M. Karam, "Slow wave propagation and plasticity of interstitial cells of Cajal in the small intestine of diabetic rats," *Exp Physiol,* vol. 96, pp. 1039-1048, 2011.

[15] P. Du, G. O'Grady, J. A. Windsor, L. K. Cheng, and A. J. Pullan, "A tissue framework for simulating the effects of gastric electrical stimulation and in vivo validation," *IEEE Trans Biomed Eng,* vol. 56, pp. 2755-2761, 2009.

[16] C. F. Code and J. H. Szurszewski, "The effect of duodenal and mid small bowel transection on the frequency gradient of the pacesetter potential in the canine small intestine," *J Physiol,* vol. 207, pp. 281-289, 1970.

[17] D. F. van Helden, D. R. Laver, J. Holdsworth, and M. S. Imtiaz, "Generation and propagation of gastric slow waves," *Clin Exp Pharmacol Physiol,* vol. 37, pp. 516-524, 2010.

[18] V. S. Tharayil, M. M. Wouters, J. E. Stanich, J. L. Roeder, S. Lei, A. Beyder, P. J. Gomez-Pinilla, M. D. Gershon, L. Maroteaux, S. J. Gibbons, and G. Farrugia, "Lack of serotonin 5-HT2B receptor alters proliferation and network volume of interstitial cells of Cajal in vivo," *Neurogastroenterol Motil,* vol. 22, pp. 462-469, 2010.